ELSEVIER

Catalysis Today 79–80 (2003) 275–283

CATALYSIS TODAY

www.elsevier.com/locate/cattod

HdPro: a mathematical model of trickle-bed reactors for the catalytic hydroprocessing of oil feedstocks

Dimitrios G. Avraam*, Iacovos A. Vasalos

Chemical Processes Engineering Research Institute, Centre for Research and Technology, P.O. Box 361, GR 570 01, Thermi, Thessaloniki, Greece

Abstract

A steady-state model for trickle-bed reactors was developed, primarily concerning hydroprocessing of light oil feedstocks containing volatile compounds. The case of a homogeneous plug flow fixed bed reactor with axial dispersion was considered. Catalyst particles were assumed to be isothermal and isoconcentrational. Mass balances, overall two-phase flow momentum balance and phase energy balances were written in detail. Hydrodynamic flow of the two phases and specifically the flow regime under which the bed was operated, the liquid holdup, the wetting efficiency of the solid particles, the two-phase flow pressure drop and the gas–liquid and liquid–solid interfacial areas were all predicted using carefully selected industrial engineering correlations.

In addition, all necessary thermophysical properties, such as phase densities, viscosities, conductivities, diffusivities, interfacial tension, latent heats of vaporization, specific heats, and molar partial enthalpies were continuously calculated as functions of the system pressure, temperature and phase composition. A suitable numerical package was developed for this kind of calculations. Phase equilibrium was calculated with the aid of the same package and the non-ideal phase behavior was taken into account, as well. Mass transfer rates were calculated by the effective diffusivity method.

Compared to a set of experimental data taken from the operation of a pilot scale hydrodesulfurization plant, excellent agreement was found. A user-friendly interface was developed to facilitate the use of the numerical package.

Keywords: Modeling; Trickle-bed reactor; Mass transfer; Thermophysical properties; Hydrodynamic flow; Volatile oil fractions; Hydroprocessing

1. Introduction

Operation of trickle-bed reactors is marked by the simultaneous presence of two phases, a gaseous and a liquid one, flowing over and through a third catalyst solid phase. Modeling of three-phase reactors has shown substantial developments recently, though it is very demanding in combining transport phenomena and heterogeneous reaction processes [1–3]. In the present paper, a steady-state model of three-phase trickle flow fixed bed reactors is presented, suitable for the case of liquid phases containing volatile compounds. The motivation for this work comes from certain commercial applications in the oil refineries concerning processing of light oil fractions with hydrogen, like hydrodesulfurization and hydrogenation. In those cases, the liquid phase holdup varies along the reactor because of partial volatilization of the lighter oil fractions. A fundamental understanding of the underlying phenomena and, especially, the interaction between mass, momentum and heat transport phenomena and heterogeneous catalysis is warranted.

* Corresponding author.
E-mail address: dgavraam@cperi.certh.gr (D.G. Avraam).

0920-5861/03/$ – see front matter
doi:10.1016/S0920-5861(03)00050-6

Nomenclature

a	interfacial area per unit volume of reactor
c	concentration
c	specific heat (Eqs. (9) and (10))
D	effective diffusivity
h	holdup
H	enthalpy
$\bar{H}$	molar partial enthalpy
H	Henry's constant
k	conductivity
k	mass transfer coefficient (Eqs. (14), (16) and (17))
K	equilibrium constant
K	mass transfer coefficient (Eq. (14))
L	reactor length
M	molecular weights
N	molar flux
N_C	number of components
N_{GR}	number of heterogeneous reactions on the gas–solid interface
N_{LR}	number of heterogeneous reactions on the liquid–solid interface
P	pressure
q	heat flux
r	reaction rate
T	temperature
v	mean phase velocity
x	mole fraction
z	axial coordinate

Greek letters

α	heat transfer coefficient
ε	porosity
η	efficiency coefficient
μ	bulk phase viscosity
ν	stoichiometric coefficient
ρ	bulk phase density

Subscripts and superscripts

A	total aromatics concentration
b	bulk phase
B	bed
E	excess property
G	gas phase
GS	gas–solid interface
GL	gas–liquid interface
i	species number
in	inlet conditions
iG	internal gas property
iL	internal liquid property
I	interface
j	reaction number
L	liquid phase
LS	liquid–solid interface
R	residual property
s	solid phase (catalyst)
W	reactor wall
$*$	molar mean quantity

For simplicity, plug flow conditions and uniform pellet properties were assumed. This means that either internal mass and heat transfer limitations are negligible or the kinetic parameters are determined using industrial scale catalyst particles. Therefore, internal mass and heat transfer rates are included in the kinetic models. On the other hand, substantial effort was made to include the non-ideal behavior of the flowing phases at the high temperature and pressure conditions of the process as well as to include mass and heat transport phenomena, which are enhanced considerably by the presence of the volatile compounds. To this end, the detailed mass, momentum and heat balances were written and solved for each compound in the liquid and the gas phase. In addition, a suitable numerical package was developed for the evaluation of the thermophysical properties of oil compounds and mixtures and for the detailed calculation of interfacial mass transfer rates, using effective diffusivity method and gas–liquid equilibrium at the interface. All variables of the system were considered to be functions of (dimensionless) space variable. On one hand, this permitted the accurate calculation of the local values of the independent system variables, i.e. phase temperatures, pressure and compositions along the reactor. On the other hand, the physicochemical properties of the phases and the hydrodynamic characteristics of the bed were correlated directly with the local values of the system variables. Moreover, the flow regime under which the bed was operated, the liquid holdup, the wetting efficiency of the solid particles, the two-phase flow pressure drop and the gas–liquid, liquid–solid and gas–solid interfacial areas were all calculated in the same manner as functions of the system variables along the reactor.

Four general chemical processes were modeled: desulfurization (HDS), denitrogenation (HDN),

saturation of olefins (HTO), and hydrogenation of mono-, di- and tri-aromatics (HTA). Reaction kinetics of the Langmuir–Hinshelwood type was used, taking into account equilibrium of aromatic hydrogenation and inhibition by hydrogen sulfide, ammonia and aromatics.

Results from the detailed model were compared with experimental data from the operation of a pilot plant unit and remarkable agreement was obtained. In view of these results, a first attempt was made to gain some insight of the complex phenomena of such processes. The agreement between theoretical and experimental data led to the development of a user-friendly interface to facilitate the use of the numerical package.

2. Theoretical

We present briefly the main equations comprising the model. Abbreviations are given below, whereas nomenclature is given at the beginning of the paper.

- Mass balance of species i in the liquid (L) bulk (b) phase:

$$\frac{\mathrm{d}N_{\mathrm{L}i}}{\mathrm{d}z} - L(N_{\mathrm{GL}i}a_{\mathrm{GL}} - N_{\mathrm{LS}i}a_{\mathrm{LS}}) = 0,$$

$$N_{\mathrm{L}i} = h_{\mathrm{L}}v_{\mathrm{L}}^{*}c_{\mathrm{L}i}^{\mathrm{b}} - h_{\mathrm{L}}\frac{D_{\mathrm{L}}}{L}c_{\mathrm{L}}^{\mathrm{b}}\frac{\mathrm{d}x_{\mathrm{L}i}^{\mathrm{b}}}{\mathrm{d}z} \quad (1a,b)$$

- Mass balance of species i in the gas (G) bulk (b) phase:

$$\frac{\mathrm{d}N_{\mathrm{G}i}}{\mathrm{d}z} + L(N_{\mathrm{GL}i}a_{\mathrm{GL}} + N_{\mathrm{GS}i}a_{\mathrm{GS}}) = 0,$$

$$N_{\mathrm{G}i} = h_{\mathrm{G}}v_{\mathrm{G}}^{*}c_{\mathrm{G}i}^{\mathrm{b}} - h_{\mathrm{G}}\frac{D_{\mathrm{G}}}{L}c_{\mathrm{G}}^{\mathrm{b}}\frac{\mathrm{d}x_{\mathrm{G}i}^{\mathrm{b}}}{\mathrm{d}z} \quad (2a,b)$$

- Mass balance of species i in the catalyst (liquid–solid interface (s)):

$$-N_{\mathrm{LS}i}a_{\mathrm{LS}} + \rho_{\mathrm{B}}h_{i\mathrm{L}}\sum_{j=1}^{N_{\mathrm{LR}}}\nu_{\mathrm{L}ij}r_{\mathrm{L}j}(\mathbf{c}_{\mathrm{L}i}^{\mathrm{s}})\eta_{\mathrm{L}j} = 0 \quad (3)$$

- Mass balance of species i in the catalyst (gas–solid interface (s)):

$$-N_{\mathrm{GS}i}a_{\mathrm{GS}} + \rho_{\mathrm{B}}h_{i\mathrm{G}}\sum_{j=1}^{N_{\mathrm{GR}}}\nu_{\mathrm{G}ij}r_{\mathrm{G}j}(\mathbf{c}_{\mathrm{G}i}^{\mathrm{s}})\eta_{\mathrm{G}j} = 0 \quad (4)$$

- Relations between phase holdups in the bed and the catalyst, respectively:

$$h_{\mathrm{L}} + h_{\mathrm{G}} = \varepsilon_{\mathrm{B}}, \qquad h_{i\mathrm{L}} + h_{i\mathrm{G}} = \varepsilon_{i} \quad (5a,b)$$

- Total mass balance of liquid phase in terms of molar and mass mean velocity:

$$h_{\mathrm{L}}v_{\mathrm{L}}^{*}c_{\mathrm{L}}^{\mathrm{b}} = \sum_{i=1}^{N_{\mathrm{C}}}N_{\mathrm{L}i}, \quad h_{\mathrm{L}}v_{\mathrm{L}}\rho_{\mathrm{L}} = \sum_{i=1}^{N_{\mathrm{C}}}M_{i}N_{\mathrm{L}i} \quad (6a,b)$$

- Total mass balance of gas phase in terms of molar and mass mean velocity:

$$h_{\mathrm{G}}v_{\mathrm{G}}^{*}c_{\mathrm{G}}^{\mathrm{b}} = \sum_{i=1}^{N_{\mathrm{C}}}N_{\mathrm{G}i}, \qquad h_{\mathrm{G}}v_{\mathrm{G}}\rho_{\mathrm{G}} = \sum_{i=1}^{N_{\mathrm{C}}}M_{i}N_{\mathrm{G}i} \quad (7a,b)$$

- Momentum balance given in the general form of correlations used hereby:

$$-\frac{\mathrm{d}P}{\mathrm{d}z}, h_{\mathrm{L}}, h_{i\mathrm{L}}, a_{\mathrm{GL}}, a_{\mathrm{LS}}, a_{\mathrm{GS}} = f(v_{\mathrm{L}}, v_{\mathrm{G}}, \mathbf{x}, \mathbf{y}, T_{\mathrm{L}}, T_{\mathrm{G}}, P) \quad (8a,b,c,d,e,f)$$

where $\mathbf{x}$, $\mathbf{y}$ are the vectors of phase properties and structural properties of catalyst and bed, respectively.

- Energy balance of liquid phase, in terms of enthalpy flux:

$$\frac{\mathrm{d}(h_{\mathrm{L}}v_{\mathrm{L}}^{*}c_{\mathrm{L}}^{\mathrm{b}}H_{\mathrm{L}})}{\mathrm{d}z} - L(q_{\mathrm{GL}}a_{\mathrm{GL}} - q_{\mathrm{LS}}a_{\mathrm{LS}} - q_{\mathrm{LW}}a_{\mathrm{LW}}) = 0,$$

$$H_{\mathrm{L}} = \sum_{i=1}^{N_{\mathrm{C}}}x_{\mathrm{L}i}^{b}\left(H_{f,\mathrm{L}i}^{0} + \int_{T_{\mathrm{ref}}}^{T_{\mathrm{L}}}c_{\mathrm{P}\,\mathrm{L}i}\,\mathrm{d}T\right) + H_{\mathrm{L}}^{\mathrm{E}} \quad (9)$$

- Energy balance of gas phase, in terms of enthalpy flux:

$$\frac{\mathrm{d}(h_{\mathrm{G}}v_{\mathrm{G}}^{*}c_{\mathrm{G}}^{\mathrm{b}}H_{\mathrm{G}})}{\mathrm{d}z} + L(q_{\mathrm{GL}}a_{\mathrm{GL}} + q_{\mathrm{GS}}a_{\mathrm{GS}} + q_{\mathrm{GW}}a_{\mathrm{GW}}) = 0,$$

$$H_{\mathrm{G}} = \sum_{i=1}^{N_{C}}x_{\mathrm{G}i}^{\mathrm{b}}\left(H_{f,\mathrm{G}i}^{0} + \int_{T_{\mathrm{ref}}}^{T_{\mathrm{G}}}c_{\mathrm{P}\,\mathrm{G}i}\,\mathrm{d}T\right) + H_{\mathrm{G}}^{\mathrm{R}} \quad (10)$$

- Energy balance of the catalyst (liquid–solid interface (s)) at steady state:

$$q_{\mathrm{LS}} = \alpha_{\mathrm{L}}^{\mathrm{s}}(T_{\mathrm{L}} - T_{\mathrm{L}}^{\mathrm{s}}) + \sum_{i=1}^{N_{\mathrm{C}}} N_{\mathrm{LS}i}\bar{H}_{\mathrm{L}i} = 0 \qquad (11)$$

- Energy balance of the catalyst (gas–solid interface (s)) at steady state:

$$q_{\mathrm{GS}} = \alpha_{\mathrm{G}}^{\mathrm{s}}(T_{\mathrm{L}} - T_{\mathrm{L}}^{\mathrm{s}}) + \sum_{i=1}^{N_{\mathrm{C}}} N_{\mathrm{GS}i}\bar{H}_{\mathrm{G}i} = 0 \qquad (12)$$

- Heat transfer rate through liquid–gas interface:

$$q_{\mathrm{GL}} = \alpha_{\mathrm{L}}(T_{\mathrm{I}} - T_{\mathrm{L}}) + \sum_{i=1}^{N_{\mathrm{C}}} N_{\mathrm{GL}i}\bar{H}_{\mathrm{L}i}$$

$$= \alpha_{\mathrm{G}}(T_{\mathrm{G}} - T_{\mathrm{I}}) + \sum_{i=1}^{N_{\mathrm{C}}} N_{\mathrm{GL}i}\bar{H}_{\mathrm{G}i} \qquad (13a,b)$$

- Mass transfer rate through liquid–gas interface:

$$N_{\mathrm{GL}i} = K_{\mathrm{GL}i}\left(\frac{c_{\mathrm{G}i}^{\mathrm{b}}}{H_i} - c_{\mathrm{L}i}^{\mathrm{b}}\right),$$

$$K_{\mathrm{GL}i} = \frac{1}{(1/k_{\mathrm{L}i}) + (1/k_{\mathrm{G}i}H_i)} \qquad (14a,b)$$

- Local equilibrium assumption at the liquid–gas interface:

$$H_i = \frac{c_{\mathrm{G}}^{\mathrm{b}} x_{\mathrm{G}i}^{\mathrm{s}}}{c_{\mathrm{L}}^{\mathrm{b}} x_{\mathrm{L}i}^{\mathrm{s}}} = \frac{c_{\mathrm{G}}^{\mathrm{b}}}{c_{\mathrm{L}}^{\mathrm{b}}} K_i(x_{\mathrm{L}i}^{\mathrm{b}}, x_{\mathrm{G}i}^{\mathrm{b}}, T_{\mathrm{I}}, P) \qquad (15)$$

- Mass transfer rate from liquid phase to solid catalyst surface:

$$N_{\mathrm{LS}i} = k_{\mathrm{LS}i}(c_{\mathrm{L}i}^{\mathrm{b}} - c_{\mathrm{L}i}^{\mathrm{s}}) \qquad (16)$$

- Mass transfer rate from gas phase to solid catalyst surface:

$$N_{\mathrm{GS}i} = k_{\mathrm{GS}i}(c_{\mathrm{G}i}^{\mathrm{b}} - c_{\mathrm{G}i}^{\mathrm{s}}) \qquad (17)$$

- Kinetic expressions of heterogeneous chemical reaction rates:
  - Hydrodesulfurization:

$$r_{\mathrm{HDS}} = \frac{a_1 k_{11}^{\mathrm{E}} c_{\mathrm{L},\mathrm{H}_2}^{\mathrm{s}} c_{\mathrm{L,S}}^{\mathrm{s}}}{(1 + K_{1,\mathrm{H_2S}}^{\mathrm{HDS}} c_{\mathrm{L},\mathrm{H_2S}}^{\mathrm{s}} + K_{1,\mathrm{A}}^{\mathrm{HDS}} c_{\mathrm{L,A}}^{\mathrm{s}})^2} + \frac{(1-a_1)k_{21}^{\mathrm{E}} c_{\mathrm{L},\mathrm{H}_2}^{\mathrm{s}} c_{\mathrm{L,S}}^{\mathrm{s}}}{(1 + K_{2,\mathrm{H_2S}}^{\mathrm{HDS}} c_{\mathrm{L},\mathrm{H_2S}}^{\mathrm{s}} + K_{2,\mathrm{A}}^{\mathrm{HDS}} c_{\mathrm{L,A}}^{\mathrm{s}})^2} \qquad (18a)$$

  - Hydrodenitrogenation:

$$r_{\mathrm{HDN}} = \frac{\beta_1 k_{12}^{\mathrm{E}} c_{\mathrm{L},\mathrm{H}_2}^{\mathrm{s}} c_{\mathrm{L,N}}^{\mathrm{s}}}{(1 + K_{1,\mathrm{H_2S}}^{\mathrm{HDN}} c_{\mathrm{L},\mathrm{H_2S}}^{\mathrm{s}} + K_{1,\mathrm{A}}^{\mathrm{HDN}} c_{\mathrm{L,A}}^{\mathrm{s}})^2} + \frac{(1-\beta_1)k_{22}^{\mathrm{E}} c_{\mathrm{L},\mathrm{H}_2}^{\mathrm{s}} c_{\mathrm{L,N}}^{\mathrm{s}}}{(1 + K_{2,\mathrm{H_2S}}^{\mathrm{HDN}} c_{\mathrm{L},\mathrm{H_2S}}^{\mathrm{s}} + K_{2,\mathrm{A}}^{\mathrm{HDN}} c_{\mathrm{L,A}}^{\mathrm{s}})^2} \qquad (18b)$$

    where

$$k_{ij}^{\mathrm{E}} = k_{ij,0}\gamma\, \mathrm{e}^{-(E_{ij}/R)(1/T - 1/T_0)} \qquad (18c)$$

$$K_{i,\mathrm{H_2S}}^{\mathrm{HDS}} = K_{i,\mathrm{H_2S}}^{\mathrm{HDN}} = K_{i,\mathrm{H_2S},0}\, \mathrm{e}^{-660/RT} \qquad (18d)$$

$$K_{i,A}^{\mathrm{HDS}} = K_{i,A}^{\mathrm{HDN}} = K_{i,A,0}\, \mathrm{e}^{-7800/RT} \qquad (18e)$$

    and α_1, β_1 are the fractions of reactive sulfur and nitrogen compounds, respectively, here taken as unity or nearly so, and γ is a feed factor depending on feed type and feed average molecular weight, taken also as unity in the absence of any other information. All other kinetic data are given in Table 1.
  - Hydrogenation of olefins:

$$r_{\mathrm{HTO}} = k_{\mathrm{HTO}}\, \mathrm{e}^{-E_{\mathrm{HTO}}/RT} c_{\mathrm{L,O}}^{\mathrm{s}} \qquad (18f)$$

  - Hydrogenation of aromatics:

    We consider hydrogenation of aromatic, A_1, to a totally or partially saturated compound, A_2 (see Table 1):

$$A_1 + \alpha H_2 \rightleftarrows A_2$$

$$r_{\mathrm{HTA}} = -\frac{k_{\mathrm{H}}^{\mathrm{E}}}{K_{\mathrm{I}}} c_{\mathrm{L},A_1}^{\mathrm{s}} + \frac{k_{\mathrm{D}}^{\mathrm{E}}}{K_I} c_{\mathrm{L},A_2}^{\mathrm{s}} \qquad (18g)$$

$$k_{\mathrm{H}}^{\mathrm{E}} = k_{\mathrm{H}} P_{\mathrm{H}_2}^{x}\, \mathrm{e}^{-(E/R)(1/T - 1/T_0)} \qquad (18h)$$

$$k_{\mathrm{D}}^{\mathrm{E}} = \frac{k_{\mathrm{H}}}{K_{\mathrm{P}} P_{\mathrm{H}_2}^{a-x}}\, \mathrm{e}^{-(E - \Delta H/R)(1/T - 1/T_0)} \qquad (18i)$$

$$K_{\mathrm{I}} = 1 + K_{\mathrm{H_2S}} P_{\mathrm{H_2S}} \qquad (18j)$$

    The kinetic data for the hydrogenation of mono-, di- and tri-aromatics are given in Table 1, as well.

- Thermophysical properties of flowing phases:

$$\text{Liquid phase}: \quad \rho_{\mathrm{L}}, \mu_{\mathrm{L}}, D_{\mathrm{L}}, c_{\mathrm{P,L}}, k_{\mathrm{L}} = f(x_{\mathrm{L}i}^{\mathrm{b}}, T_{\mathrm{L}}, P) \qquad (19)$$

Table 1
Kinetic and thermodynamic data

HDS	HDN	HTO
$k_{11,0} = 11.75\,h^{-1}$	$k_{11,0} = 5.756\,h^{-1}$	$k_{HTO} = 187.5\,h^{-1}$
$k_{21,0} = 2.0\,h^{-1}$	$k_{21,0} = 0.374\,h^{-1}$	$E_{HTO} = 39957200$ J/kg mol
$E_{11} = 75324840$ J/kg mol	$E_{11} = 79077600$ J/kg mol	
$E_{21} = 75324840$ J/kg mol	$E_{21} = 62760000$ J/kg mol	
$K_{H_2S,0} = 2.8\,atm^{-1}$	$K_{H_2S,0} = 2.8\,atm^{-1}$	
$K_{A,0} = 0.38\,atm^{-1}$	$K_{A,0} = 0.38\,atm^{-1}$	
$T_0 = 561$ K	$T_0 = 638$ K	

Hydrogenation of aromatics

Species	α	x	k_H (1/s)	K_P	T_0 (°C)	E (kJ/mol)	$-\Delta H$ (kcal/mol)
Mono-∅ → O	3	1.8	4.6×10^{-4}	5.4×10^{-3}	350	667.4	52.3
Di-∅∅ → ∅O	2	1.5	9×10^{-3}	1.4×10^{-2}	350	667.4	33.6
Tri-∅∅∅ → OOO	7	0.1	7.3×10^{-1}	4.7×10^{-10}	350	667.4	106.1

$$\text{Gas phase}: \quad \rho_G, \mu_G, D_G, c_{P,G}, k_G = f(x^b_{Gi}, T_G, P) \tag{20}$$

$$\gamma_{GL} = f(x^b_{Li}, x^b_{Gi}, T_I, P) \tag{21}$$

- Correlations and thermodynamic models:

  The following correlations were used, whereas only the corresponding literature references are given below for the sake of brevity: a_{GL}, a_{LS}, a_{GS} [4], h_L [5], $-(dP/dz)$ [6], D_L, D_G [7], k_{Li}, K_{LSi} [8], k_{Gi} [9], K_{GSi} [10].

  The modified constitutive equation RKS (Redlich–Kwong–Soave) [11] was used for the calculation of liquid–gas equilibrium at the interface and molar partial enthalpies of gas and liquid phases. Moreover, the heat transfer coefficients were estimated from the mass transfer coefficients using the Chilton–Colburn analogy [12]. The multicomponent diffusivities were computed from the diffusion coefficients at infinite dilution according to Vignes [13] and Wilke–Chang [14] equations, as it is recommended by the American Petroleum Institute (API) numerical methods. Also, various numerical methods recommended by the API were adopted for the calculation of pure substances and phase physicochemical properties, as it is dictated in Eqs. (19)–(21). The raw data were the critical properties of the pure substances, T_{ci}, P_{ci}, V_{ci}, accentric factors, ω_i, radii of gyration, R_g, etc. Finally, kinetic expressions of Langmuir–Hinshelwood type were carefully chosen from the literature, whereas efficiency and pellet wetting coefficients were taken to be unity.

- Danckwerts boundary conditions:

$$(N_{Li})_{z=0} = h_{L,in} v^*_{Li,in} c^b_{Li,in}, \quad \left(\frac{dc^b_{Li}}{dz}\right)_{z=1} = 0, \ i = 1, 2, \ldots, N_C \tag{22}$$

$$(N_{Gi})_{z=0} = h_{G,in} v^*_{Gi,in} c^b_{Gi,in}, \quad \left(\frac{dc^b_{Li}}{dz}\right)_{z=1} = 0, \ i = 1, 2, \ldots, N_C \tag{23}$$

$$(E_{Li})_{z=0} = h_{L,in} v^*_{Li,in} c^b_{Li,in} H_{L,in}, \quad \left(\frac{dT_L}{dz}\right)_{z=1} = 0, \ i = 1, 2, \ldots, N_C \tag{24}$$

$$(E_{Gi})_{z=0} = h_{G,in} v^*_{Gi,in} c^b_{Gi,in} H_{G,in}, \quad \left(\frac{dT_G}{dz}\right)_{z=1} = 0, \ i = 1, 2, \ldots, N_C \tag{25}$$

$$(P)_{z=1} = P_{out} \tag{26}$$

The problem at hands is a boundary value problem, which needs suitable treatment. Collocation on finite elements aided by a method for solving extended systems of non-linear algebraic equations was used successfully. A total number of five finite elements and second-degree polynomials as trial functions were adequate for accuracy better than 10^{-5}.

3. Results and discussion

Hydroprocessing of a very light diesel feedstock was studied. An inert pseudocomponent corresponding to the C_{17} fraction of diesel was used in the model to match the physical properties of the real feedstock. The composition of the liquid feed is presented in Table 2. Pure hydrogen comprised the gas feed.

Fig. 1 presents the steady-state mass fraction distribution of the main compounds along the reactor, as computed by the model. The operational conditions were: $T = 340\,^{\circ}C$, $P = 30$ bar, WHSV (wetting hourly space velocity) $= 2\,h^{-1}$, H_2/oil = 1000 SCFB (standard cubic feed of hydrogen per barrel of oil feed). Fig. 2 presents the distribution of phase temperature, holdup and pressure along the reactor. Since an adiabatic reactor is modeled and all individual reactions are exothermic, axial phase temperature profiles are increasing functions. However, the increase in the phase temperatures along the reactor is limited by the

Table 2
Composition (wt.%) of oil feedstock

Compound	wt.%
Sulfur compounds	3.67
Nitrogen compounds	0.88
Olefins	30.00
Mono-aromatics	24.60
Di-aromatics	8.20
Tri-aromatics	4.10
C_{17}	28.54
Hydrogen	0.00

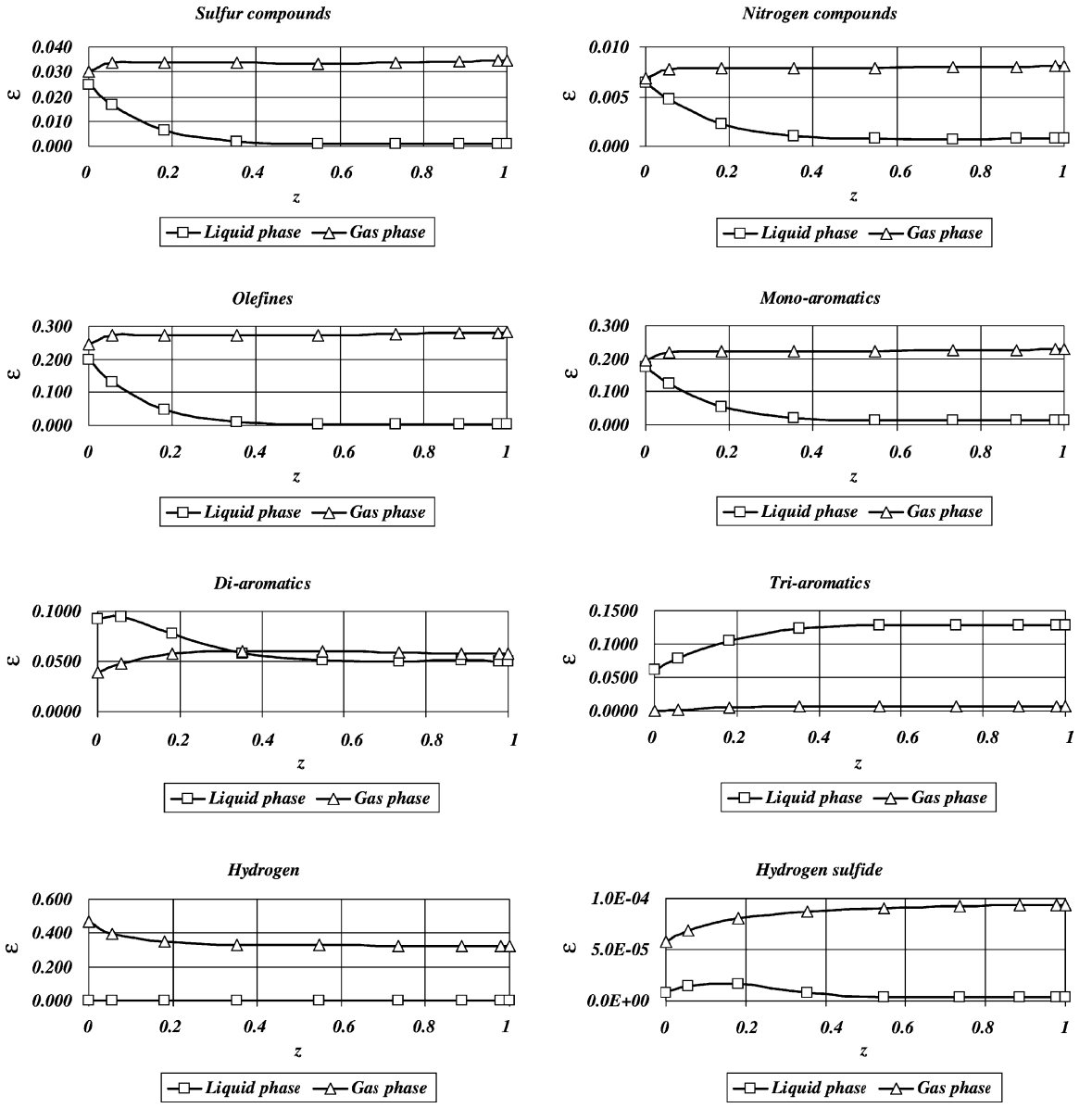

Fig. 1. Distribution of mass fraction of the main compounds, at steady state.

volatilization of the lighter oil fractions, which consumes a considerable amount of the heat produced by the reactions. Along the last half of the reactor, the phase temperatures are stabilized since reactions take place mainly at the inlet zone of it. This is due to the high activity of the fresh catalyst. Catalyst deactivation was not modeled in the present study. Fig. 2 shows also a reduction of the liquid holdup, which accompanies the excessive volatilization of the lighter oil feedstock fractions. Gas holdup increases accordingly.

Fig. 3 presents experimental and theoretical values of the conversion of sulfur compounds in the feedstock as a function of the residence time and the inlet temperature. Traditionally, such data are presented in

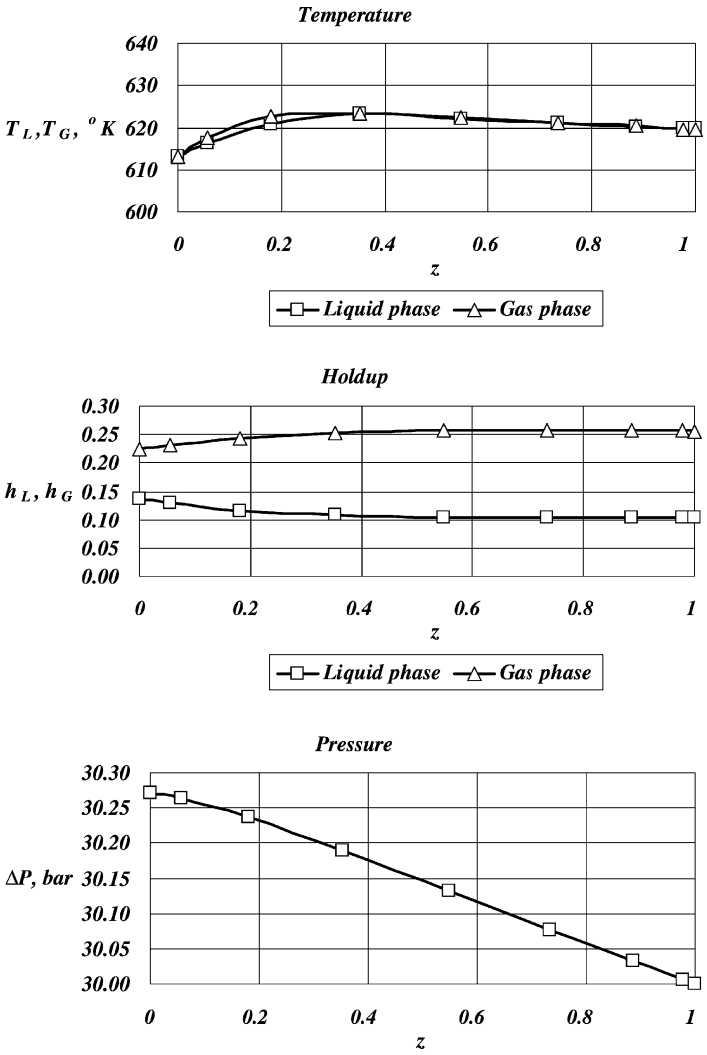

Fig. 2. Distribution of phase temperature, holdup and pressure, at steady state.

the form of sulfur residual percentage in the product as a function of the reciprocal WHSV at different values of inlet temperature. A set of experimental tests was performed in the pilot scale HDS plant, using as feedstock the light diesel of Table 2. The values of the inlet temperature and the WHSV were systematically varied, whereas inlet pressure and gas to oil feed ratio were kept constant ($P = 30$ bar, H_2/oil=1000 SCFB). All other operational parameters were kept constant, whereas the most important bed and catalyst properties are presented in Table 3. We run a similar set of theoretical simulations under the same operational parameters. The simulator effectively modeled the diesel feedstock. Open symbols represent the experimental results, whereas solid symbols represent the theoretical values. Qualitative as well as quantitative agreement between the theoretical and the experimental values is excellent. Moreover, as inlet temperature increases at constant WHSV or WHSV decreases (i.e. reciprocal WHSV increases) at constant temperature removal of sulfur compounds from the oil feedstock is intensified and less sulfur remains in the product. This is an important environmental target for future fuels.

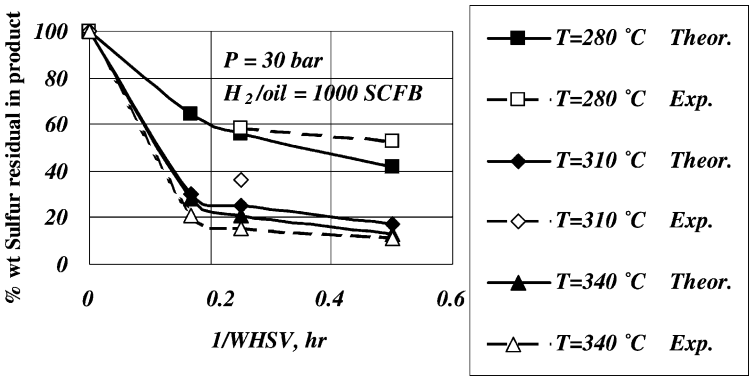

Fig. 3. Sulfur residual in the product as a function of the reciprocal wetting hourly space velocity.

Table 3
Main operational parameter values[a]

Bed		Catalyst	
Diameter (cm)	3	Extrudate shape	Trilobe
Length (cm)	17.5	Nominal size (mm)	1.2
Catalyst load (g)	20	Cobalt (wt.% dry basis)	3.1
Dilution (alumina) (g)	151	Molybdenum (wt.% dry basis)	12.4
Porosity (%)	36.13	Surface area (m^2/g)	250
		Pore volume (cm^3/g)	0.53
		Reactor loading density (kg/m^3)	610
		Compacted bulk density (kg/m^3)	700

[a] Oil feedstock—feedstock: diesel MOH; specific gravity: 0.8676 g/cm^3.

4. Conclusions

A steady-state model for trickle-bed reactors was developed to model hydroprocessing of light oil feedstocks that contain considerable amounts of volatile compounds. The main conclusions are:

- Hydroprocessing of oil feedstocks in catalytic fixed bed reactors under trickling conditions can be modeled effectively using fundamental principles of reaction engineering, transport phenomena, thermodynamics and by suitable calculation of the thermophysical properties of mixtures of oil compounds that form the flowing liquid and gas phases.
- Volatility of the light oil compounds should be taken into account. Liquid holdup decreases along the reactor, whereas gas holdup increases accordingly due to the volatility of the lighter compounds of the feedstock. Therefore, phase properties vary along the reactor, as well.
- As the inlet temperature increases removal of sulfur compounds from the oil feedstock increases, with all other operational parameters kept constant.
- As WHSV decreases (i.e. reciprocal WHSV increases) removal of sulfur compounds from the oil feedstock increases, with all other operational parameters kept constant.

References

[1] S. Toppinen, J. Aittamaa, T. Salmi, Chem. Eng. Sci. 51 (1996) 4335.
[2] J. Wärnå, T. Salmi, Comput. Chem. Eng. 20 (1996) 39.
[3] M.R. Khadilkar, P.L. Mills, M.P. Dudukovic, Chem. Eng. Sci. 54 (1999) 2421.
[4] J.C. Charpentier, Chem. Eng. J. 11 (1976) 161.
[5] F. Larachi, A. Laurent, N. Midoux, G. Wild, Chem. Eng. Sci. 46 (1991) 1233.
[6] M.J. Ellman, N. Midoux, A. Laurent, J.C. Charpentier, Chem. Eng. Sci. 43 (1988) 2201.
[7] J.M. Hochmann, E. Effron, I&EC Fund. 8 (1969) 63.
[8] S. Goto, J.M. Smith, AIChE J. 21 (1975) 706.
[9] A. Gianetto, V. Specchia, G. Baldi, AIChE J. 19 (1973) 916.
[10] W. Yaïci, A. Laurent, N. Midoux, J.C. Charpentier, Ind. Chem. Eng. 28 (1988) 299.
[11] M.S. Graboski, T.E. Daubert, Ind. Eng. Chem. Process Des. Dev. 17 (1978) 443.
[12] T.H. Chilton, A.P. Colburn, Ind. Eng. Chem. 26 (1934) 1183.
[13] A. Vignes, Ind. Eng. Chem. Fund. 5 (1966) 189.
[14] C.R. Wilke, P. Chang, AIChE J. 1 (1955) 264.